ALGERIAN DEMOCRATIC AND POPULAR REPUBLIC MINISTRY OF

HIGHER EDUCATION AND SCIENTIFIC RESEARCH

Mohamed El-Bachir El-Ibrahimi University - Bordj Bou Arreridj

Faculty of Science and Technology

Department of Electronics

Master's Thesis

Presented to obtain

MASTER'S DEGREE

FIELD: ELECTRONICS

Mendoud Riad

Saha Islam

Title

Energy gaps and optical properties for the ternary semiconductor alloys $In_xGa_{1-x}N$

Defended on: 01 / 07 / 2025

Name & Surname	Grade	Role	Institution
Dr . L .DIB	**MCB**	**Chairman**	**Univ-BBA**
Dr . F.Fares	**MCA**	**Supervisor**	**Univ-BBA**
Dr. A. DJEMOUAI	**MCB**	**Examiner**	**Univ-BBA**

Academic Year 2024/2025


بسم الله الرحمن الرحيم

Thanks

First of all we thank Almighty God for giving us the privilege and chance to study and follow the path of science and knowledge after years.

We extend our sincere thanks to our supervisor, Professor Mrs. F. FARES, for her understanding, advice and valuable help.

We would also like to thank all the Professors for their kindness and effective guidance.

We also extend our deep gratitude to all the professors of the University of BORDJ BOUARRERIDJ, particularly those of the ELECTRONICS department.

Finally, we thank all the people, near or far, who contributed to the development of this thesis.

Thanks to everyone

Table of Contents

List of Figures

List Of tables:

General Introduction

General introduction:

The use and understanding of materials with special properties has fueled technological innovation, introducing countless instruments and tools into our environment that hold electronic mysteries. Among these are semiconductors, which are key materials in today's technology, given the richness of their behavior in relation to the stresses to which they are subjected. However, they are the materials of choice for optoelectronics, enabling electrons to be controlled for the detection, modulation and emission of light, in other words, they are used to make optical components and systems [1].

The physical properties of semiconductor materials can be enhanced by the use of ternary semiconductor alloys of the $A_xB_{1-x}C$ form, which offer the advantage of independent control of the crystalline parameter and bandgap width [1].

On the theoretical side, electronic structure calculation methods can provide important complementary data to experimental work. Calculations based on the empirical pseudopotential method (E.P.M.), combined with the virtual crystal approximation, are the simplest and fastest. III-V semiconductors have attracted much attention for their potential application in infrared optical devices [2].

III-V semiconductors and their corresponding alloys currently occupy a privileged position in many applications such as optoelectronics. The field of optoelectronics has seen considerable growth thanks to the use of direct-gap III-V semiconductor materials ($In_xGa_{1-x}N$ and associated alloys) [3].

Our dissertation is devoted to the study of the electronic, optical and dielectric properties of ternary $In_xGa_{1-x}N$ type III-V semiconductor alloys crystallizing in the zinc-blende structure. The aim of the work is to investigate the parameters of the electronic band structure, namely energy gaps, refractive index and static dielectric constant. We have divided this manuscript into three chapters:

- The first chapter we presented some general information on the physical properties of semiconductors.
- The second chapter is devoted to methods for calculating the electronic energy band structure included the pseudopotential method, which is a powerful calculation tool in solid-state physics.

- The third chapter deals with the practical aspects of this work. The main results obtained will be presented, along with their interpretation and a comparison with other theoretical and experimental findings. Finally, a general conclusion will be provided.

Chapter I: General Concepts of Semiconductors

I. SEMICONDUCTORS

semiconductor is a material that exhibits electrical characteristics intermediate between those of an insulator and those of a conductor. Although it is generally considered an insulator, a semiconductor offers a non-negligible probability that an electron will contribute to electrical conductivity [4]. In other words, its conductivity is lower than that of conductors but higher than that of insulators. Thus, semiconductors occupy an intermediate zone, offering unique possibilities for the manipulation of electric current [5].

The energy band theory is commonly used to model the electrical behavior of semiconductors. According to this theory, semiconductors have a relatively narrow bandgap, allowing electrons from the valence band to easily transition to the conduction band [6]. When an electric potential is applied across the semiconductor, a small electric current is produced [6]. This current is caused by the movement of electrons toward the conduction band and by the "holes" left behind in the valence band [7].

Thus, semiconductors allow electrical conduction through the mobility of electrons and holes induced by the application of an electric potential [8].

The control of the electrical conductivity of semiconductors can be achieved through doping, that is, by adding small amounts of impurities into the material to create an excess or deficiency of electrons [9]. By bringing differently doped semiconductors into contact, junctions can be formed, allowing the regulation of the direction and intensity of the electric current flowing through the device. This fundamental characteristic is used in the operation of modern electronic components such as diodes, transistors, and many others. Thus, doping and the creation of junctions in semiconductors play an essential role in controlling and utilizing electric current for the design of various electronic devices.

I.1.1 The Different Types of Semiconductors:

I.1.1.1 Intrinsic Semiconductor:

An intrinsic semiconductor is a semiconductor that has not been intentionally doped with impurities. These semiconductors are extremely pure and possess a highly ordered crystal structure, with a perfectly periodic lattice. Moreover, their impurity level is very low, with fewer

than one impurity atom per 10^{13} atoms of the semiconductor element [5]. This ensures that the electrical properties of the intrinsic material are primarily determined by its crystal structure and the characteristics of the electrons in its valence band and conduction band. Intrinsic semiconductors are used as a reference to study the fundamental properties of semiconductors and to evaluate the effect of dopants on their conductivity and electronic properties [5].

The figure below provides a general overview of intrinsic semiconductors in terms of band structure and charge carrier distribution [10].

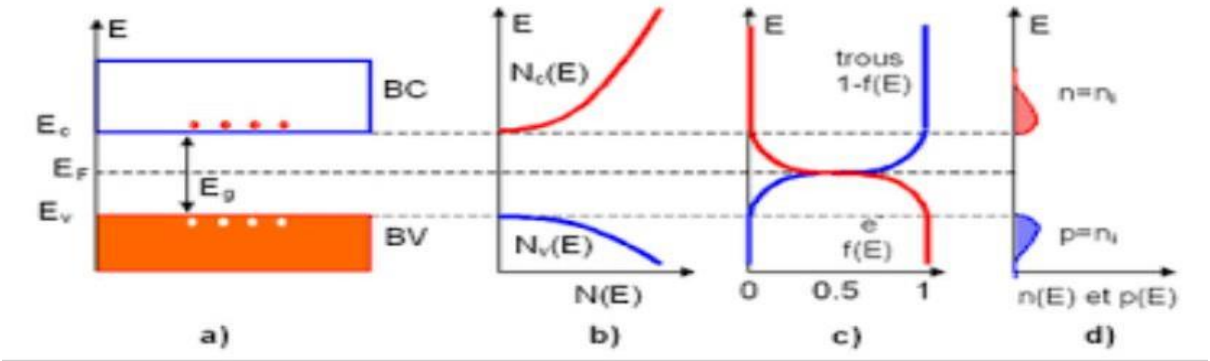

Figure I.1: Intrinsic Semiconductor

a) Energy Band Diagram

b) Energy Density of States

c) Fermi-Dirac Distributions

d) Energy Distributions of Carriers (n and p carrier densities correspond to the shaded areas)

I.1.1.2 Extrinsic Semiconductor:

In intrinsic or pure semiconductors, the concentration of electrons and holes at normal temperatures is very low. As a result, to achieve a noticeable current density through the semiconductor, a strong electric field must be applied.

This limitation can be overcome by introducing suitable impurities into intrinsic semiconductors. Extrinsic semiconductors are those in which a significant amount of impurities is present [5].

In general, the impurities can be elements from either group III or group V of the periodic table. Based on the type of impurity added, extrinsic semiconductors are classified into two categories: n-type semiconductors and p-type semiconductors [7].

a. P-Type Semiconductors:

A p-type semiconductor is an intrinsic semiconductor (e.g., silicon Si) into which acceptor- type impurities (e.g., boron B) have been introduced. These impurities are called acceptors because they accept an electron from the valence band in order to form a bond within the semiconductor crystal.

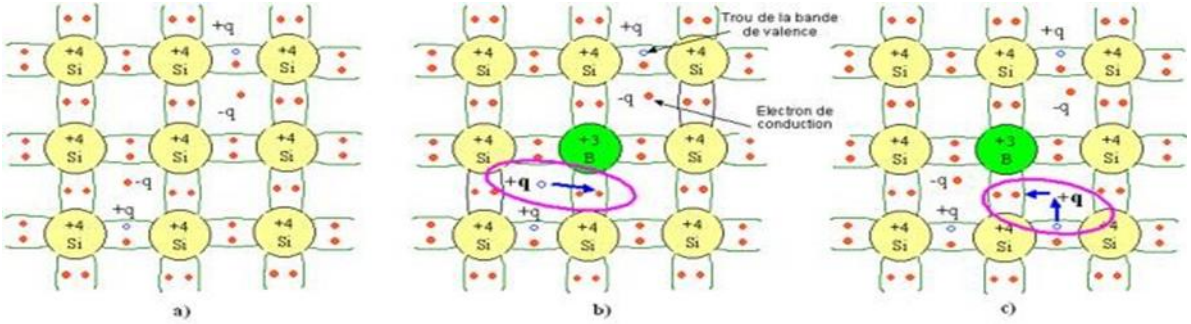

Figure I.2: P-Type Semiconductors

b. N-Type Semiconductors:

An n-type semiconductor is an intrinsic semiconductor (e.g., silicon Si) into which donor-type impurities (e.g., arsenic As) have been introduced. These impurities are called donors because they donate an electron to the conduction band in order to form a bond with the semiconductor crystal.

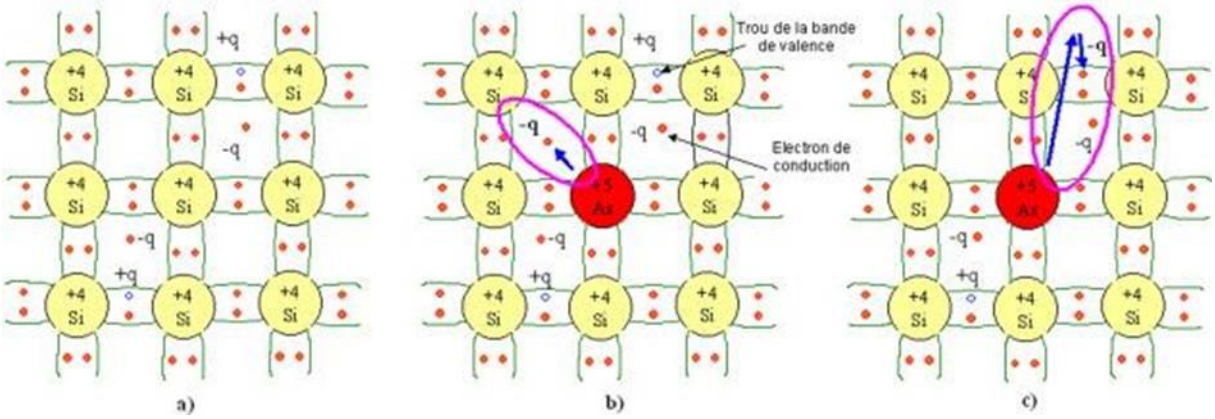

Figure I.3 : N-Type Semiconductors

I.1.2 Semiconductor Materials:

The family of semiconductors is very large. Semiconductors are classified according to their chemical composition. There are:

a. Simple Intrinsic Semiconductors:

A simple intrinsic semiconductor is made of a single element, such as the semiconductors from Group IV of the periodic table, for example, silicon (Si) and germanium (Ge).

b. Compound Intrinsic Semiconductors:

In this category, the semiconductor is composed of at least two different types of atoms. Binary semiconductors from the (II-VI) class consist of an element from Group II and another element from Group VI of the periodic table. Semiconductors from the (III-V) class are composed of an element from Group III and another element from Group V of the periodic table. Conductors from the (IV-VI) class are also included.

There are also other types of semiconductors composed of three different atoms (ternary) or even four atoms (quaternary).

I.2 Semiconductors Group III and Group V :

The advances made by chemists, materials physicists and technologists have played a crucial role in the research and manufacture of new materials, particularly alloys [8]. Numerous binary, ternary and quaternary alloys have been created thanks to their efforts. These advances are made possible

by the transfer of electronic charges between Group III and Group V atoms, giving these materials unique properties [5].

This study focuses on the analysis of the electronic properties of III-V semiconductor compounds using the local pseudopotential method. These compounds are formed by elements from groups III and V of the periodic table, and generally exhibit properties similar to those of group II-VI and IV semiconductors [11]. Most III-V semiconductors are characterized by a band gap greater than 1 eV [5]. From this perspective, III-V semiconductors such as GaAs, and their alloys, are potentially more efficient and more resistant to cosmic radiation than silicon, for two obvious reasons: their gap is direct and wider [12].

I.3. The main advantages of III-V semiconductors :

are as follows

Thanks to their semi-insulating nature (SI substrate), these compounds are ideal for the manufacture of microwave integrated circuits.

-Their ability to withstand radiation is another notable feature.

Their ability to operate at high temperatures is of great importance in military applications.

-Their performance in terms of speed and power consumption is far superior to that of computers using silicon circuits, making them ideal for digital applications.

-Another important advantage lies in the III-V semiconductor's ability to generate terahertz (THz) waves in the far-infrared region of the electromagnetic spectrum. This unique and valuable capability makes it possible to generate THz waves in a compact, room-temperature device.

I.4 The Electronic Properties of Semiconductors:

The band structure of semiconductors plays a crucial role in their electronic properties, and the width of the band gap defines their level of conductivity. Over the decades, considerable efforts have been made to accurately determine, both theoretically and experimentally, the band structures of different semiconductor materials. These studies aim to understand in detail the energy levels of electrons and holes in the valence and conduction bands, as well as to assess the conduction properties and specific electronic characteristics of semiconductors. Determining the band

structure of a semiconductor is an extremely complex challenge. This is primarily due to the lack of an analytical expression that allows for direct calculation of the potential energy.

At T = 0 K, this band is completely filled with electrons in a perfect semiconductor. The remaining four antibonding orbitals give rise to four upper bands that form the conduction band, which is empty and separated from the valence band by an energy gap of width Eg. In direct band gap semiconductors [13], the maximum of the valence band and the minimum of the conduction band are located at the Γ point.

Electronic energy band structure:

Energy bands indicate the possible energy states for electrons as a function of their wave vector. They are therefore represented in reciprocal space and, for simplicity, in the directions of highest symmetry of the first Brillouin zone. They are divided into valence bands and conduction bands. It is the lowest valence band and the highest conduction band, and the band gap that separates them, that primarily determine the transport properties of the semiconductor. [14]

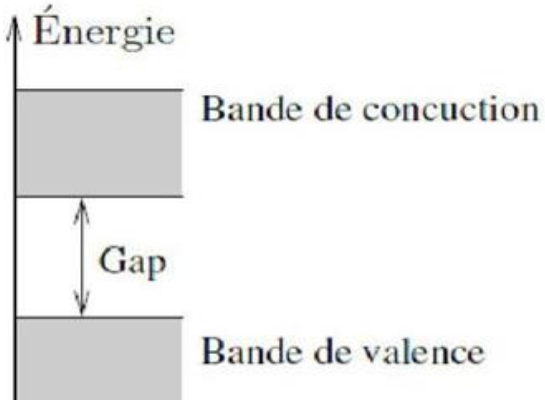

Figure I.4: Representation of the conduction and valence bands.

I.4.1 Energy Gap:

The gap is by definition the width of the band gap, that is, the energy difference between the absolute minimum of the conduction band and the absolute maximum of the valence band. Therefore, there are two fundamental types of semiconductors: direct gap semiconductors and indirect gap semiconductors.

I.4.1.1 Direct gap:

A semiconductor is a direct band gap semiconductor if the valence band maximum and the conduction band minimum correspond to the same wave vector K. (The central conduction band minimum corresponds to electrons with low effective mass, and therefore very mobile).

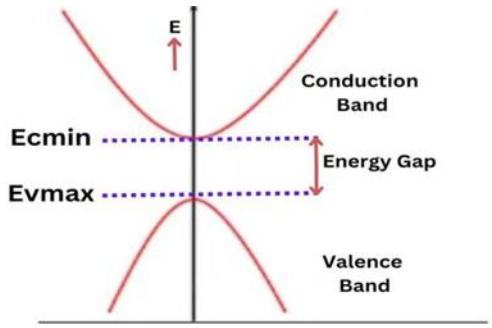

Figure I. 5 : Representation of the direct band gap

I.4.1.2 Indirect gap:

Indirect gap semiconductors, in which the minimum of the conduction band and the maximum of the valence band are located at different points in k-space (their conduction band corresponds to electrons with a high effective mass, and therefore low mobility).

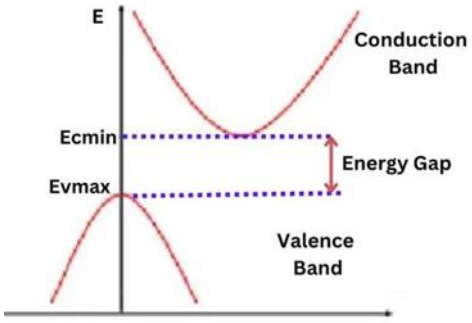

Figure I. 6: Representation of the indirect band gap

I.4.2 Network constant:

In crystallography, the lattice constant (often denoted a) defines the distance between atoms in crystal lattices. It is an indicator of structural compatibility between different materials, and can be determined by X-ray diffraction.

Experiments show that the lattice constant of ternary alloys is determined by the average of the lattice constants of their binary constituents. This relationship follows Vegard's law..

Ternary alloy $A_xB_{1-x}C$

$$\mathbf{a(x)=x\cdot a_{AC} + (1-x)\cdot a_{BC}} \quad \text{(I.1)}$$

a(x) : is the lattice constant of the ternary alloy. a_{AC} : is the lattice constant of the compound AC..

a_{BC} : is the lattice constant of the compound BC.

Indium Gallium Nitride (InGaN, $In_xGa_{1-x}N$) is a semiconductor material made from a mixture of Gallium Nitride (GaN) and Indium Nitride (InN) [15]. It is a III-V ternary compound with a direct bandgap. Its bandgap width can be tuned by varying the amount of indium in the alloy.

The lattice parameters of $In_xGa_{1-x}N$ can be derived from the parameters of GaN and InN through linear interpolation [12,16].

Such as:

$$a(In_xGa_{1-X}N) = x.a(InN)+(1 - x).a(GaN) \quad \text{(I.2)}$$

where a (in Å) is the lattice parameter of $In_xGa_{1-X}N$.

I.5.Alloy Theory:

Semiconductor alloys have attracted great interest over the past three decades, especially for studying the variation of their energy band gaps as a function of their composition.

Their use in microelectronics and optoelectronics has motivated researchers to deepen both theoretical and experimental investigations.

Consequently, various crystal growth techniques such as vapor-phase epitaxy, liquid- phase epitaxy, the floating zone Bridgman technique, and the Czochralski method have been employed [17].

I.5.1. The Theory of a Ternary Alloy:

Semiconductor alloys have revolutionized the applications of semiconductor devices by providing intrinsic solutions to adjust the bandgap, thus enabling the optimization and expansion of their uses. Among these alloys, III-V semiconductors have opened new perspectives and have been the foundation of advanced generations of devices over the past decades, significantly increasing the possibilities for engineering material propertiesinterest due to their potential in electro-optic applications. Specifically, their use in areas such as high-efficiency light-emitting diodes and high-speed switching devices has been extensively explored. [18]

The energy bandgap is a crucial parameter for optoelectronic devices, as it is closely related to the operating wavelength. Therefore, studying the dependence of the fundamental energy gap on alloy composition is of particular importance in this context.

I.6 The virtual crystal approximation:

In studying the physical properties of ternary alloys, the Virtual Crystal Approximation (VCA) is commonly used, with or without compositional disorder. However, recent experimental and theoretical studies on various semiconductor alloys suggest that VCA reaches its limits when the difference in electronic properties between the constituent atoms exceeds a critical threshold. This anomaly is typically attributed to the effects of compositional disorder, which is not accounted for in the VCA. As a result, There is growing interest in understanding the "bowing" factor, i.e., the deviation from the Virtual Crystal Approximation (VCA), by relating it to the properties of the individual components [18].

Cohen and Chelikowsky provide further details on this. In their study, the nonlinear least squares method was used to optimize the parameters of empirical pseudopotentials. [17]

For the case of the VCA, the physical properties are given by the following equation:

$$FAxB1\text{-}xC(x) = X\ FAC + (1\text{-}x)\ FBC \qquad (I.3)$$

For example, the lattice parameter of the ternary alloy AxB1-xC will be:

$$a\ AxB1\text{-}xC(x) = xaAC + (1\text{-}x)\ aBC \qquad (I.4)$$

and the form factors:

$$V_{S,A}(G) = x\ V_{S,A}(G) = (1\text{-}x)\ V_{S,A}(G) \qquad (I.5)$$

Taking into account the effect of disorder, the form factors of the ternary system are given by the following expression:

$$V_{S,A}(G) = xV_{AC}(G) + (1\text{-}x)V \qquad (I.6)$$

Or the adjustable parameter ppp, which stimulates the effect of disorder, has a value of 0 in the VCA alone and is treated as a tunable parameter once compositional disorder is taken into account.

$$F_{A_XB_{1-X}C}(X) = XF_{AC} + (1 - X)F_{BC} \qquad (I.7)$$

For example, the lattice parameter of the ternary alloy AxB1-xC

$$aA\text{-}B1\text{-}xC(x) = xaAC + (1\text{-}x)\ a\ BC \qquad (I.8)$$

And the form factors:

$$V^{S,A}(G) = xV_{AC}^{S,A}(G) + (1 - x)V_{BC}^{SAA}(G) \qquad (I.9)$$

Taking into account the effect of disorder, the form factors of the ternary system are given by the following expression:

$$V^{S,A}(G) = xV_{AC}^{S,A}(G) + (1 - x)V_{BC}^{S,A}(G) - p[x(1 - x)]^{\frac{1}{2}}\left[V_{AC}^{S,A}(G) - V_{BC}^{S,A}(G)\right] \qquad (I.10)$$

Where the adjustable parameter p, which stimulates the effect of disorder, has a value of 0 in the VCA alone and is treated as a tunable parameter once compositional disorder is taken into account.

The interest of element III nitrides in optoelectronics:

Element III nitrides (GaN, AlN, InN and their alloys) are semiconductors with remarkable properties. The most important is undoubtedly the low forbidden energy gap of InN (0.7 eV) [7]. This extends the spectral coverage of nitrides, which now extends from the far ultraviolet with AlN (6.2 eV, or 200 nm) [9], to the mid-infrared with InN (0.7 eV, or 1770 nm), through the near

ultraviolet with GaN (3.39 eV, or 365 nm) [10], and the visible spectrum with InGaN or AlInN alloys.

I.7 Evolution of the Physical Properties of $In_xGa_{1-x}N$:

I.7.1 Bandgap Energy:

According to Vegard's law, the variation of the bandgap energy of the $In_xGa_{1-x}N$ alloy as a function of its composition is not linear but follows a quadratic-type relationship [19].

$$Eg(InxGa1–XN) = x.\ Eg(InN) + (1 — x)Eg(GaN) — b.x(1 — x) \quad (I.11)$$

In this equation, the curvature parameter b, called the bowing parameter, is approximately 1.43 eV for the $In_xGa_{1-x}N$ alloy [19].

The values of the bandgap energies for the pure materials are:

Eg(InN) = 0,7 eV [19]

Eg(GaN) = 3,42 eV . [20]

x: Stoichiometric coefficient evaluated x corresponds to the amount of indium incorporated into the gallium nitride.

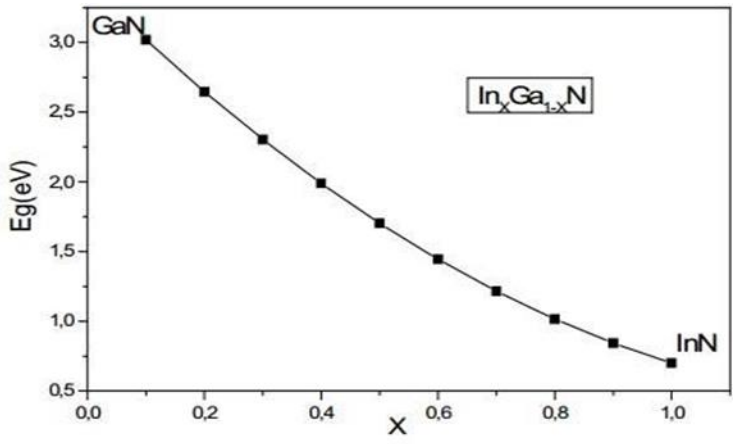

Figure I.7: Evolution of the Ban dgap Width as a Function of x. **[21]**

Technologically, the more indium is incorporated into gallium, the lower the bandgap energy of the InGaN ternary alloy decreases.

Lattice parameter of the InxGa(1-x)N alloy as a function of x:

The lattice parameter of the ternary alloy varies according to VEGARD's law, which is a linear function of the composition x of the parent binary compounds of the ternary alloy, on a:

$$a\ (InxGa(1-x)N) = x.\ aIn + (1-x)\ aGaN \qquad (I.12)$$

Where aIn and aGaN represent the lattice parameters of the binary bodies constituting the material.Table (I-5) summarizes the nitride parameters.

Le tableau représente la différence entre les valeurs expérimentales et theoriques des prametres de maille des deux nitrures.

The table represents the difference between the experimental and theoretical values of the lattice parameters of the two nitrides

Materiaux	The lattice parameters	Experimental value
GaN	**4.50**	**4.5**
In	**4.957**	**4.98**

Table I. 1: the oretical and experimental Lattice parameter a **. [21]**

I.7.2 Electron Affinity :

The evolution of the electron affinity χchiχ as a function of the stoichiometric coefficient is given by the relation [22] :

$$\chi\ (InGaN) = x.\chi(InN) + \chi(GaN).(1 — x) \qquad (I.13)$$

With the affinities: χ(InN) =5.8 eV [23]

χ(GaN) = 4.1 eV [24]

I.7.3 Electron and Hole Masses :

The masses of electrons and holes as a function of the stoichiometric coefficient x are given by the following relation [28]:

me, t (InxGa1−xN)) = x.me, t (InN) + (1-x).me, t (GaN) Where:

me : Electron mass (me (GaN) /m0 =0.2, me (InN) /m0 =0.05) [25]. mt : Hole mass (mt (GaN) /m0 =1.25, mt (InN) /m0 =0.6) [25].

I.7.4 Refractive Index :

The evolution of the refractive index with the stoichiometric coefficient x is given by the relation [26]:

n(InxGa1–xN) = x. n(InN) + (1 — x) n (GaN) (I.14)

Or

n(InxGa1–xN) = 2.506 + 0.91.x (I.15)

I.7.5 Dielectric Constant (or Electric Permittivity)

The evolution of the dielectric constant with the stoichiometric coefficient x is given by the relation [27]:

εr (InxGa1-xN) = 4.33.x + 10.28

I.7.6 Absorption Coefficient

A material's ability to absorb light radiation is generally measured by its absorption coefficient.

The latter is an indispensable parameter when designing optoelectronic components such as photovoltaic cells photovoltaic cells, photodiodes and photodetectors in general. Fig. shows the evolution of the absorption coefficients as a function of the stoichiometric coefficient x is given by the relation [26] :

$$\alpha(\lambda) = C(h\frac{C}{\lambda} - Eg)^{1/2} = C.(hv - Eg)^{1/2} \quad (I.16)$$

Where:

λ : Wavelength ν : frequency

C : Constant for the InGaN semiconductor InGaN =2,2.10 5 cm-1 h: Planck's constant

c : Speed of light

Eg : Band gap of InGaN

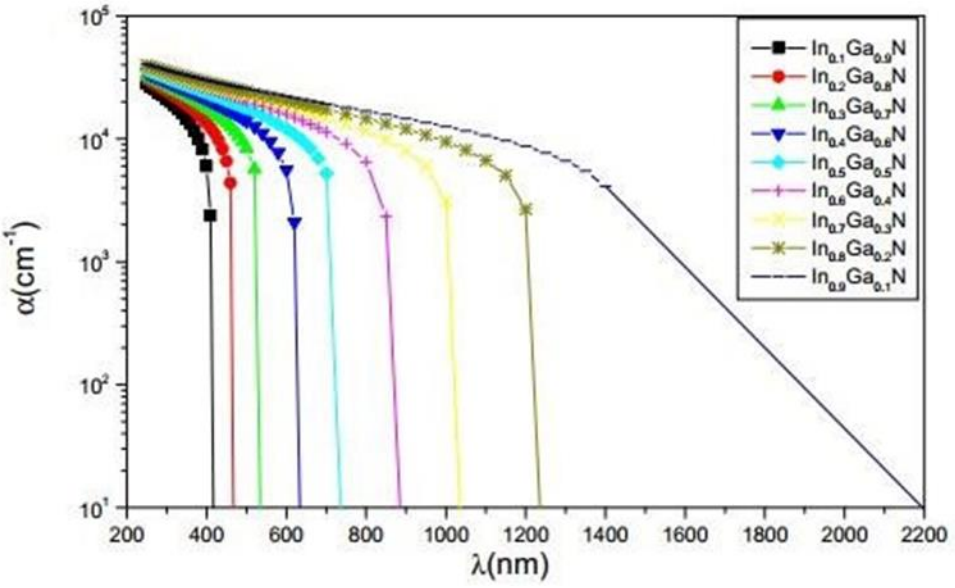

Figure I.8: Evolution of the Absorption Coefficient as a Function of Wavelength for Different Values of x **[21]**.

I.8. Optical Properties:

I.8.1 The Refractive Index :

The refractive index n of a medium indicates how the speed of light (or other waves) is reduced in this medium at a specific wavelength.

When light passes through an interface between two different materials, it undergoes a change in direction based on the ratio of the refractive indices of these materials.

The refractive index n of semiconductors is of fundamental importance in various electronic devices such as photonic crystals, waveguides, solar cells, and detectors. Accurate knowledge of this index is essential for the design, characterization, and optimization of these devices [5].

I.9. Crystal Structure :

The crystalline state is distinguished from other solid states by the fact that atoms are arranged in a defined and ordered manner. This state is generated by the periodic repetition of atoms or groups of atoms (of the same or different types), known as the crystal motif or unit cell, along the three spatial directions. This periodic translation produces the crystal structure. The result is an ordered assembly of nuclei and electrons, bound together primarily by Coulomb forces [4].

I.9.1. Zinc Blende (ZB) Structure :

Most binary semiconductor materials have a Zinc Blende (ZB) structure.

This structure, which is similar to that of diamond, consists of two interpenetrating face- centered cubic (FCC) sublattices.

As shown in Figure I-5, the zinc blende unit cell corresponds to a face-centered cubic lattice in which all non-contiguous tetrahedral sites are occupied, resulting in a multiplicity of 8 atoms per unit cell (an equal number of cations and anions).Since the roles of the two ions are symmetric, the zinc blende structure can be viewed as two interpenetrating face-centered cubic sublattices, displaced by one quarter of the cube's body diagonal. One sublattice is occupied by anions (P, As, or Sb), and the other by cations (Al, Ga, or In). [4]

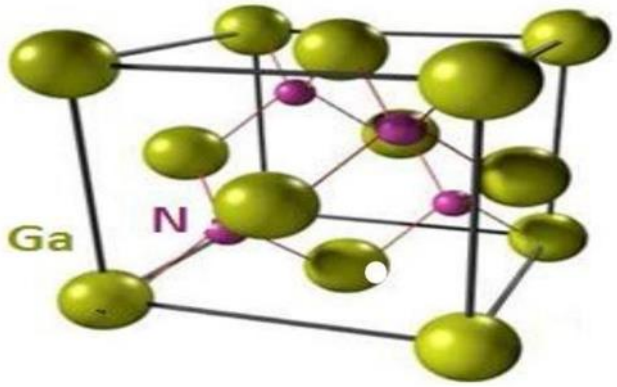

Figure I. 9: Crystal lattice of the zinc-blende structure.

I.9.2. The Lattice Constant

The lattice constant is defined as the distance separating two consecutive unit cells, denoted by a [28]. Determining the lattice constant is the first step in characterizing the structure of a crystal.

Knowing the lattice constant allows the calculation of the atomic density and, consequently, the electronic density.

The lattice constant can vary depending on temperature and pressure [29].

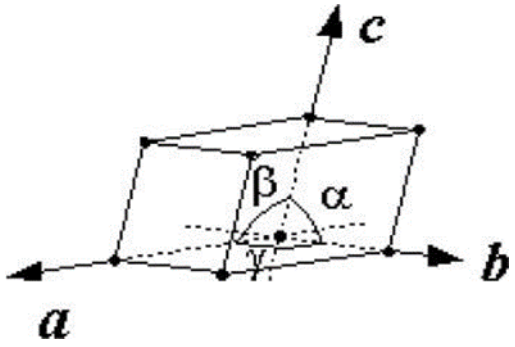

Figure I.10: Primitive triclinic lattice in three-dimensional space.

I.10. The application of the Ternary Semiconductor Alloy $In_xGa_{1-x}N$:

The ternary alloy $In_xGa_{1-x}N$, belonging to the III-group nitrides family, has recently marked a major breakthrough in the field of ultraviolet lighting, profoundly transforming lighting technologies. These materials are distinguished by their robustness: they withstand high doses of radiation while retaining excellent optoelectronic properties. By modulating the indium composition, the bandgap can be adjusted to cover a wide portion of the electromagnetic spectrum, ranging from ultraviolet to visible light. This flexibility makes $In_xGa_{1-x}N$ alloys particularly well-suited for many optoelectronic applications, including light-emitting diodes (LEDs) and laser diodes.

The electronic band structure of these alloys varies depending on the indium composition. The dependence of the bandgap energy on x is generally nearly linear, evolving between the values of the binary materials GaN and InN. Calculations performed using the plane-wave pseudopotential method have shown that both GaN and InN exhibit a direct bandgap, localized at the symmetry point along high-symmetry directions in the Brillouin zone. [6]

The advantages of III-V semiconductors:

The main advantages of III-V semiconductors are as follows:

- Their semi-insulating properties (due to the Si substrate) allow the fabrication of microwave integrated circuits.

- Their high resistance to radiation makes them suitable for use in harsh environments, such as space applications.

-Their ability to operate at higher temperatures than standard silicon, which is important for military applications.

-Their speed/power consumption performance is significantly higher than that of computers using silicon circuits (digital applications).

-Their very wide frequency range, extending from 1 GHz to over 100 GHz.

The III-V compound sector is the only microwave sector whose technology is currently mature enough for industrial production. This maturity and its development have therefore made it possible to achieve affordable production costs, which nevertheless remain significantly higher than those of the silicon sector.

Group III nitride semiconductors are of critical importance for applications in power electronics and high-frequency devices.

microelectronics and optoelectronics in the blue and ultraviolet spectral ranges (LEDs, lasers, photodetectors), due to their exceptional electronic, physical, and optical properties.

Gallium nitride GaN is a wide direct bandgap semiconductor (3.4 eV), very promising for applications in micro- and optoelectronics. When combined with other III-V compounds, it can be

used to create various devices such as colored or white LEDs (light-emitting diodes) for signaling, color displays, or lighting, blue or violet LDs (laser diodes) for printing (laser) or optical data storage (CDs and DVDs), solar-blind UV detectors for missile identification or guidance, fire detection, or personal UV dosimeters.

I.11. Conclusion:

In this first chapter, we provided a general overview of III-V semiconductor materials and their applications. We also introduced key concepts such as energy band gaps and reciprocal lattices, followed by a description of the $In_xGa_{1-x}N$ ternary alloy. Finally, we focused on the evolution of the optical properties of $In_xGa_{1-x}N$ as a function of the stoichiometric coefficient *x*.

Chapter II Methods For Calculating Energy Bands

II.1. Introduction

Understanding the electronic structure is essential for explaining the physical and chemical properties of materials. However, calculating the electronic structure of a crystal requires solving the many-body problem involving numerous nuclei and electrons, making an exact solution of the Schrödinger equation practically impossible.

In this chapter, we present the Empirical Pseudopotential Method (EPM), a semi-empirical approach closely related to *ab initio* methods. It serves as a powerful tool for predicting the structural and electronic properties of materials and, in most cases, yields highly satisfactory results.

II.2. Schrödinger Equation

Solving the Schrödinger equation for such a system is extremely difficult, as stated by Dirac in 1929:

$$H\psi = E\psi \qquad (II.1)$$

E: Total energy

ψ: Wave function (Eigen function). H: Hamiltonian operator [30].

The exact Hamiltonian for this system is composed of five terms: the kinetic energy of the nuclei, the kinetic energy of the electrons, as well as the various interactions between them:

$$H\ tot = Te + Tn + Vn{-}n + Vn{-}e + Ve{-}e \qquad (II.2)$$

With:

$V_{n-n} = -\Sigma_{I<J} \frac{Z_I Z_J e^2}{|\vec{R}_I - \vec{R}_J|}$: Potential energy of interaction between the nuclei

$V_{n-e} = \frac{1}{2}\Sigma_{I,i} \frac{Z_I e^2}{|\vec{r}_I - \vec{R}_J|}$: Potential energy of nucleus-electron interaction

$V_{e-e} = \frac{1}{2}\Sigma_{i<j} \frac{e^2}{|\vec{r}_I - \vec{r}_J|}$: Potential energy of repulsion between electrons

The Schrödinger equation is therefore expressed in the following form:

$$H\Psi = \left[-\sum_i \frac{h^2}{2m}\nabla_i^2 - \sum_I \frac{h^2}{2}\nabla_I^2 - \sum_{I<J} \frac{Z_I Z_J e^2}{|\vec{R}_I - \vec{R}_J|} + \frac{1}{2}\Sigma_{I,i} \frac{Z_I e^2}{|\vec{r}_i - \vec{R}_I|} + \frac{1}{2}\Sigma_{i<j} \frac{e^2}{|\vec{r}_i - \vec{r}_j|}\right]\Psi = E\,\Psi \quad \text{(II.3)}$$

To solve this equation, certain approaches are used.

II.3 Approximations:

II.3.1. The Born-Oppenheimer Approximation:

According to Born and Oppenheimer [32], the motion of the nuclei is initially neglected in comparison to that of the electrons. This is justified by the fact that the mass of the nuclei is more than three orders of magnitude greater than that of the electrons. The total Hamiltonian can then be replaced by the following electronic Hamiltonian [32].

$$H = T_e + V_{e-e} + V_{e-n} \quad \text{(II.4)}$$

The Schrödinger equation is therefore rewritten as follows:

$$H\psi e = \psi e \quad \text{(II.5)}$$

With Te and Ee: the eigenstate and Eigen energy of the system of Ne electrons.

E_{TOTALE}: The total energy of the system is then given by:

$$E_{TOTALE} = Ee + Enoy \quad \text{(II.6)}$$

Although the problem is greatly simplified, the exact solution of equation (II.6) is still impossible.

II.3.2 The Hartree Approximation :

The Hartree approximation involves seeking the eigenfunctions of the Hamiltonian HHH in an approximate form, assuming that the total wave function can be written as a product of single-particle wave functions:

$$\psi\, appro_X = \psi 1r1 \times \psi 2r2 \times \cdots\cdots\cdots \times \psi nrn) \quad \text{(II.7)}$$

This approximation is based on the free-electron assumption, meaning that both electron–electron interactions and spin effects are neglected. This leads to two major limitations: the total Coulomb

repulsion within the electronic system is overestimated, and the Pauli exclusion principle is not properly accounted for.

II.4 The Pseudopotential Method

he pseudopotential technique [33, 34, 35, 36 ,37] is a veritable revolution in band structure theory. Since its introduction, this method has proved highly effective in investigating and understanding the electronic properties of solids.

The pseudopotential was first introduced by Fermi (1934) for the study of observed atomic levels. In the following years, Hellman [38] proposed an approximation of the pseudopotential that could be used in the determination of the energy pseudopotential in alkali metals.

hus, the Phillips-Kleinman cancellation theorem [39, 40], derived from the OPW method, demonstrated that valence electrons experimentally experience a repulsive potential when they are outside the core; in other words, the wave functions of the valence electrons are constrained to be orthogonal to the core states. If this repulsive potential is added to the attractive potential of the ionic core, they nearly cancel each other out, leaving a weak attractive pseudopotential.

II.4.1.Concept of the Pseudopotential

In an atom or in a solid, the potential acting on a valence electron is highly attractive inside the core (Figure II-2-a). In this region, the wave function oscillates rapidly (Figure II-2-c), which results in high kinetic energy, while the potential energy is very low. This behavior can also be seen as a manifestation of the Pauli exclusion principle, which requires the wave function to be orthogonal to the core electron orbitals [41]

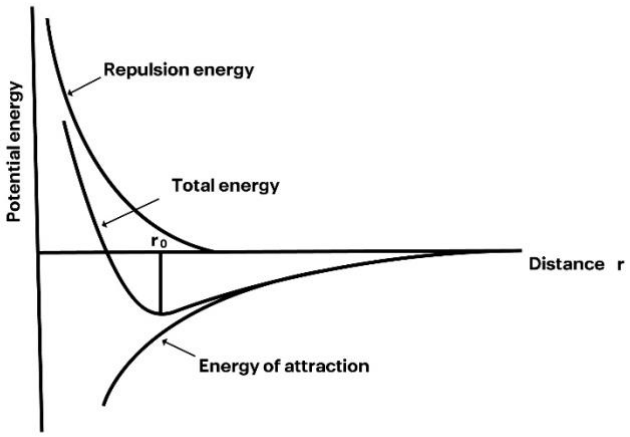

Figure II-1: Interaction potential of two atoms as a function of atomic distance.

Phillips and Kleinman [39, 40] noted that the effect of this orthogonality results in a repulsive term that tends to cancel the strong attractive potential U(r). The description of the Phillips and Kleinman theory [39, 40] is as follows: The real wave function ψ\psiψ is composed of a smooth part that can be expanded in plane waves and a part that can be expanded as a sum of core states ϕ That is to say:

$$\psi = \phi + \sum\alpha\ c\phi c \qquad \text{(II-8)}$$

Substituting this expression into the Schrödinger equation:

$$H\psi = E\psi \qquad \text{(II-9)}$$

Mathematical transformations of equation (II-1) lead us to write:

$$H\phi + \sum c\ (E - EC)\langle\phi c|\phi\rangle = E\phi \qquad \text{(II-10)}$$

In which summation extends over all saturated core states, it represents a non-local operator acting on the Φ part of the wave function. This operator is like a purely repulsive potential VR since the orthogonalization terms have the effect of holding valence electrons to the core exercise (Pauli principle).

$$VR = \sum(E - EC)\phi C\langle\phi c|\phi\rangle \qquad \text{(II-11)}$$

As a result, equation (II-10) becomes:

$$\left[\frac{P^2}{2m} + V_{PS}\right]\phi = E\phi \qquad \text{(II-12)}$$

Where:

$$V_{PS} = V_R + V_C \qquad \text{(II-13)}$$

With:

Vc: The ionic core potential, which is strong and negative, while VR is a positive repulsive potential. Their summation thus reduces the value of VPS [39], as shown in Figure (II-2-b). The smallness of VPS (pseudopotential) makes the method extremely advantageous (reducing computational complexity).

Generally, relation (II-12) is written as follows:

$$H_{PS}\phi = E\phi \qquad \text{(II-14)}$$

There are two types of pseudopotentials: the local pseudopotential (local EPM) and the non-local pseudopotential (non-local EPM), which will be discussed below.

a- The Local Pseudopotential Method :

This empirical method is widely used in the calculation of semiconductor band structures. It does not take into account the energy dependence of the pseudopotential on the angular momentum states representing the core states [42].

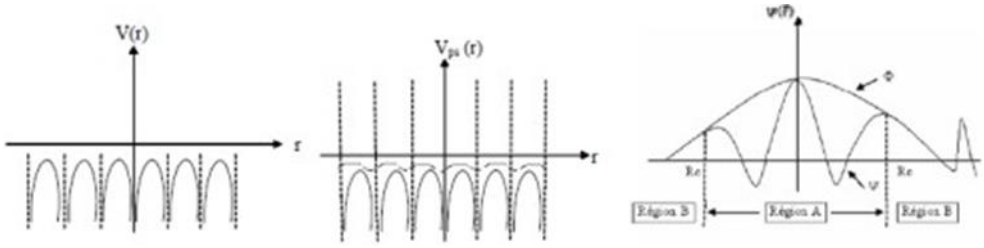

(a)crystalline potential (b) pseudopotential (c) wave function

Figure II-2: The wave function and the potential

In this approach, the wave pseudopotential of a valence electron is given by:

$$H_{PS}\phi_{nk}(r) = E_n(k)\phi_{nk}(r) \quad \text{(II.15)}$$

With:

$$H_{PS} = \frac{-h^2}{2m}\Delta + V_{PS}(r) \quad \text{(II.16)}$$

and $\emptyset nk$ is expanded on the basis of plane wave functions:

$$\phi_{nk}(r) = \sum_m C_m(k)\exp[i(k + G_m)r] \quad \text{(II.17)}$$

here the convergence is determined by the reciprocal lattice vector G, and the En are the solutions of the secular equation given by:

$$\langle\phi_G|H - E|\phi_{G'}\rangle = \langle\phi_G|H|\phi_{G'}\rangle - E_n(k)\langle\phi_G/\phi_{G'}\rangle = 0 \quad \text{(II.18)}$$

Or for:

$$H = T + V_{PS} \quad \text{(II.19)}$$

$$\langle\phi_G|H - E|\phi_{G'}\rangle = \langle\phi_G|T|\phi_{G'}\rangle + \langle\phi_G|V_{PS}|\phi_{G'}\rangle - E_n(k)\langle\phi_G/\phi_{G'}\rangle = 0 \quad \text{(II.20)}$$

With:

$$\langle\phi_G|T|\phi_{G'}\rangle = \frac{h^2}{2m}(k + G)^2\delta_{GG'} \quad \text{(II.21)}$$

So it remains to determine: $\langle\emptyset G|VPS|\emptyset G'\rangle$

$$\langle\phi_G|V_{PS}|\phi_{G'}\rangle \coloneqq \langle\phi_G|V_{PS}^{L}|\phi_{G'}\rangle + \langle\phi_G|V_{PS}^{NL}|\phi_{G'}\rangle \quad \text{(II.22)}$$

With:

$$\langle\phi_G|V_{PS}^{L}|\phi_{G'}\rangle = \frac{1}{\Omega}\int_n \exp\big(-i(k + r)\big)V(r)\exp\,(i(k + G'))d^3r$$

$$= \frac{1}{\Omega}\int_n V(r)\exp[i(G + G')r]d^3r = V(G - G')$$

Posen's $(G - G') = q$

Hence,

$$V_{PS}^{L} = \frac{1}{\Omega}\int_\Omega V(r)\exp\,(-iqr)d^3r \quad \text{(II.23)}$$

In the case of this approximation, the total pseudopotential of the crystal is assumed to be the superposition of the atomic pseudopotentials Vi at sites Rn. These pseudopotentials possess spherical symmetry.

$$V_{PS}^{L} = \sum_{n}^{m}\sum_{i}^{l} V_i(r - R_n - T_i) \qquad \text{(II.24)}$$

m: number of unit cells in the solid l: number of atoms per unit cell.

Rn: translation vector in the real lattice

Ti: position vector linking two atoms within the unit cell.

It is observed that the pseudopotential is a simple function of position, which characterizes its locality. The periodicity of the crystal allows the Fourier transform to be written in the form:

$$V(G) = \frac{1}{\Omega}\int_{\Omega} V_{PS}^{L}(r)\exp[-i(Gr)]d^3r \qquad \text{(II.25)}$$

Ω: being the volume of the crystal.

The diamond structure has two atoms per unit, so Ω = 2 N Ωa , where Ωa and N represent the atomic volume and mesh number respectively

Replacing (II-24) in (II-25) and if q = G, we end up with :

$$V(G) = \frac{1}{2N}\sum_{n}\exp[-i(G.T_i)]\frac{1}{\Omega_a}\int_{\Omega} V_i(r)\exp[-i(Gr)]d^3r \qquad \text{(II.26)}$$

Since the crystalline potential is the sum of the local atomic pseudopotentials this potential can be expressed as a function of atomic form factors.

$$V_a(G) = \frac{1}{\Omega_a}\int_{\Omega} V_a(r)\, exp[-i(Gr)]d^3r \qquad \text{(II.27)}$$

These form factors can be determined from experimental optical gaps according to Cohen and Bergestresser [42], which is why this method is called empirical.

A mathematical concatenation of relation (II-26), will lead to write:

$$V(G) = \frac{1}{2}\sum_{i=1}^{2}\exp[-i(G.T_i)]V_a(G) \qquad \text{(II.28)}$$

Where the summation index i varies from 1 to 2 for type semiconductors $A^N B^{S-N}$

Finally (II-28) becomes :

$$V(\mathrm{G}) = \frac{1}{2}\{exp[-\mathrm{i}(\mathrm{GT}_1)]V_1(G) + exp[-\mathrm{i}(\mathrm{GT}_2)]V_2(G)\} \quad \text{(II.29)}$$

Where:

$V_G^S = \frac{1}{2}[V_1(G) - V_2(G)]$: Represents the symmetrical form factor.

$V_G^A = \frac{1}{2}[V_1(G) - V_2(G)]$: Represents the antisym metrical form factor. Taking these last two expressions last two expressions, relationship (II-29) becomes:

$$V(G) = \frac{1}{2}[V_G^S\{exp[-i(GT_1)] + exp[-i(GT_2)]\} + V_G^A\{exp[-i(GT_1)] + exp[-i(GT_2)]\}] \quad \text{(II.30)}$$

Where:

T1 and T2 represent the positions of the two atoms. In the case of the diamond structure, the two atoms are identical, so:

$$T_1 = T = \left(\frac{a}{8}\right)(1,1,1) \quad \text{and} \quad T_2 = -T = -\left(\frac{a}{8}\right)(1,1,1)$$

$$V_1 = V_2 = \left(\frac{1}{2}\right)V^S$$

$$V^A = 0$$

and expression (II-30) is expressed as:

$$V(G) = V_G^S \cos(G.T) + iV_G^A \sin(G.T) \quad \text{(II.31)}$$

To which:

$$\cos(G.T) = S^S(G) \quad \text{(II.32)}$$

$$\sin(G.T) = S^A(G) \quad \text{(II.33)}$$

Represent the symmetrical and antisymmetrical structure factors respectively. From the relationship:

$$V_G = \sum_\alpha S^\alpha(G)V^\alpha(G) \quad \text{(II.34)}$$

Which can be transferred to the relationship translating the pseudopotential :

$$V_{PS}^L(r) = \sum_{|G|} V(G)exp[i(G.R)] \quad \text{(II.35)}$$

Since the total pseudopotential of the crystal has been identified, the pseudowave function (II-17), which in the form of the Bloch function, allows us to write the secular equation in the following form

as follows:

$$|\frac{h^2}{2m}(k+G)^2\delta_{GG'} + V_G^S\cos(G.T) + iV_G^A\sin(G.T) - E_n(k)\delta_{GG'}|C_{nk}(G) = 0 \quad \text{(II.36)}$$

This secular equation has a solution if and only if the determinant is zero. That is to say:

$$det||H_{GG'}(k) - E_n(k)\delta_{GG'}|| \quad \text{(II.37)}$$

Or:

$$H_{GG'}(k) = -\frac{h^2}{2m}(k+G)^2\delta_{GG'} + V^\alpha(G-G')S^\alpha(G-G') \quad \text{(II.38)}$$

This secular equation converges rapidly $|G| < |G_0| = \left(\frac{2\pi}{a}\right)^{\frac{1}{2}}(11)^{\frac{1}{2}}$ from because the pseudopotential cancels out for values greater than

It is therefore sufficient to know three form factors for the diamond structure which has a center of symmetry:

$$V^S(111) = V_3^S \qquad V^S(220) = V_8^S \qquad V^S(311) = V_{11}^S$$

But for the zinc-blende structure, in addition to its form factors, we need three other antisymmetric form factors [43]:

$V^A(111) = V_3^A$ $V^A(200) = V_4^A$ $V^A(311) = V_{11}^A$

Symmetrical form factors VS, are obtained from monoatomic structures such as Ge, Si, Sn etc ... according to the Heine-Abarenkov method [37]. Whereas antisymmetric form factors are determined experimentally according to Cohe n and Bergestresser [2].

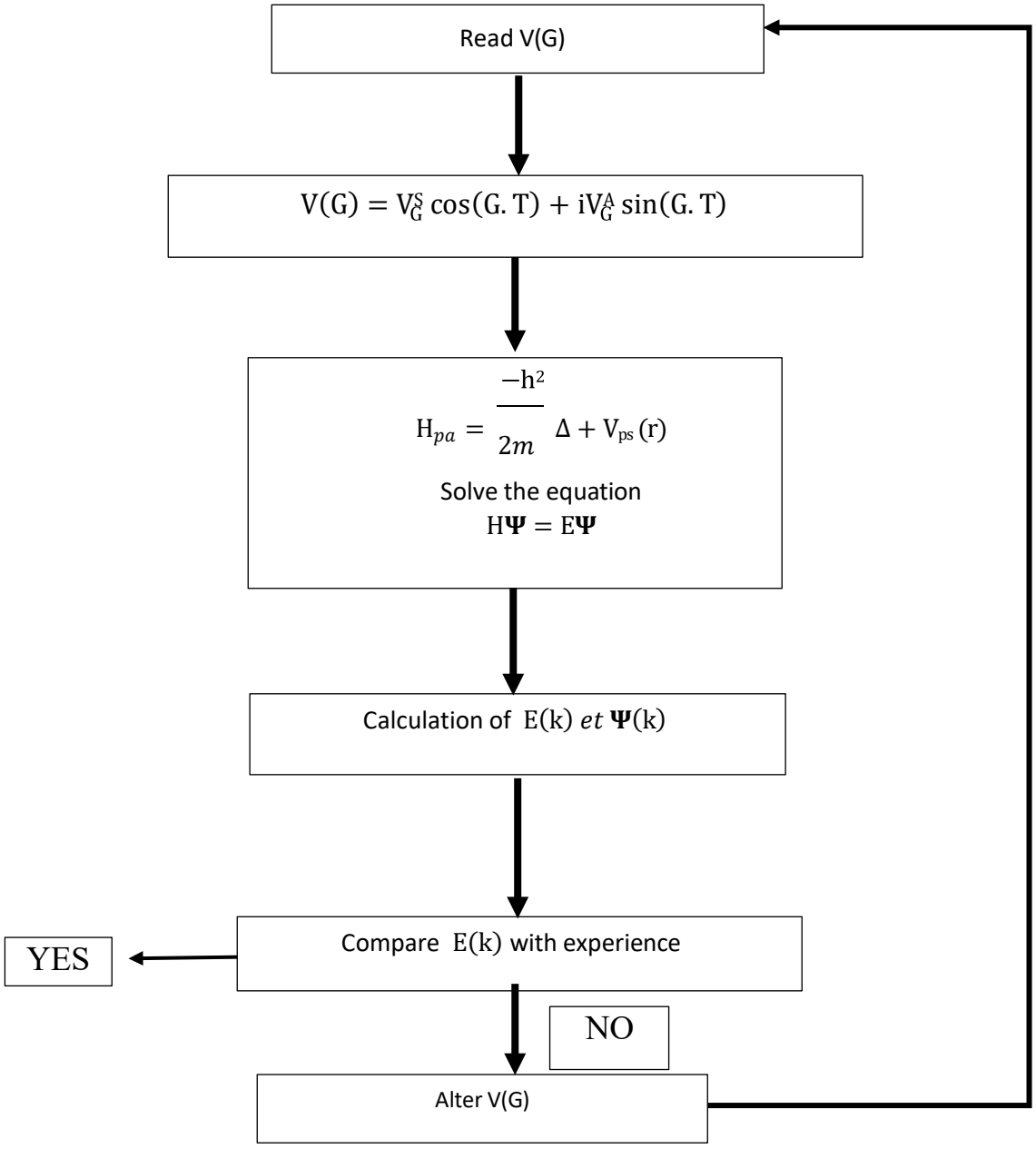

Figure II-3: block diagram of the method E.P.M local

II.5 Conclusion

We have shown how to calculate the energy band structure of these materials. The pseudo-potential approach is currently the most widely used approach for determining determining electron band structures and other properties such as the band gap.

The choice of the EPM empirical pseudo-potential method is based essentially on the fact that it is possible to obtain the electron states of a given material. on obtaining valence states without calculating core states, which are not necessary for describing necessary for describing the physical properties of a system. The actual states are described by pseudo-wave functions represented in Fourier space by a limited number of a limited number of plane waves, thus minimizing numerical calculations.

Chapter III: Results And Discussion

III.1 Introduction

A thorough understanding of the electronic and optical properties of semiconductors requires an in- depth study of the physical environment, that is to say the way in which atoms and molecules are arranged within the solid.

Scientific progress is closely linked to the development of semiconductor physics, using their properties to produce certain electronic and optoelectronic devices.

Currently, multi-component alloys have attracted a great deal of attention due to their uses as substrates, coating layers, active elements in optoelectronic devices for high-speed photonic devices, and for other applications. The operating characteristics of devices depend on the electronic properties of the constituent materials, and these properties can be enhanced by the use of ternary alloys. Ternary alloys are therefore widely used in the manufacture of electronic components. Knowledge of these properties is needed to determine their field of application.

Our work focuses on the study of the electronic , optical and dielectric properties of InxGa1-xN ternary semiconductor alloys using numerical simulation. We have opted to use the empirical pseudopotential method (EPM) coupled with the virtual crystal approximation (VCA).and we have carried out these calculations on our InN and GaN binary materials.

III.2. Study of electronic properties

The calculations are mainly based on the empirical pseudo-potential method (EPM), using the improved virtual crystal approximation (VCA) based on the zinc blende structure model. Without taking into account the effect of disorder.

In the EPM, the crystal potential is represented by a linear superposition of atomic potentials that are modified and adjusted to have the same known energy gap values at selected points in the Brillouin zone.

To find out the following parameters (band structure, energy gaps, refractive index and high-frequency dielectric constant), it is first necessary to study and determine the electronic, optical and dielectric properties of ternary InxGa1-xN semiconductor alloys.

The empirical nature of the pseudo-potential method involves adjusting the form factors, in order to achieve the closest agreement of the calculated energy levels with the theoretical values. [25]

$$V_{ps}(r) = V_{ps}^{L}(r) + V_{ps}^{NL}(r) \quad \text{(III.1)}$$

With:

$V_{ps}^{L}(r)$: Local part of the pseudopotential.

$V_{ps}^{NL}(r)$: Non-local part of the pseudopotential.

We noted that the non-local part of the pseudopotential is neglected.

The local part of the pseudopotential (also called form factors) is given as a function of the parameters of the pseudopotential, which are none other than the Fourier transform of the atomic potential inside the Wigner-Seitz cell.

$$V_{ps}(r) = V_{ps}^{L}(r) = \sum_{G} V(G)\, e^{iGr} \quad \text{(III-2)}$$

Where : V(G) is Form factor.

III.2.1 Parameters of the pseudo empirical potential V(G)

The parameters are determined by the non-linear least-squares method [26]. All parameters are optimized simultaneously under a well-defined criterion of minimizing the mean of the square root of the gap deviation (rms)

The nonlinear least squares method requires that the deviation (rms) of the energy gaps calculated by the pseudopotential method from those found experimentally be defined by [3] :

$$\delta = \left[\sum_{i,j}^{m} \frac{(\Delta E_{ij})^2}{m-n}\right]^2 \quad \text{(III-3)}$$

Where :

$$\Delta Eij = Eij^{exp} - Eij^{cal} \quad \text{(III-4)}$$

$E_{ij}^{exp}\ et\ E_{ij}^{cal}$ are respectively, the observed and calculated energies between state i with k=ki and state j with k=kj of the same pair (i,j) and n the number of parameters of the empirical pseudopotential. The initial form factor values are iteratively improved or modified until the [27] is minimized.

The form factors of the InN and GaN binary semiconductor compounds are adjusted and shown in Table (III-1).

III.2.1.1 Form factors :

In the present work, the electronic properties of ternary InxGa1-xN alloys deposited on two binary compound substrates InN and GaN are investigated.

The adjusted VS symmetrical and VA antisymmetrical pseudopotential form factors, together with the lattice parameters of the binary compounds used, are given in Table (III-1).

Binary component	Form factors						Network constants
	$V_S(3)$	$V_S(8)$	$V_S(11)$	$V_A(3)$	$V_A(4)$	$V_A(11)$	a (Å)
GaN X=0	-0.347240	-0.016	0.21217	0.159988	0.200	0.135	4.5
InN X=1	-0.172195	-0.01555	0.044698	0.238742	0.23210	-0.03149	4.98

Table III-1 : The symmetric (VS) and antisymmetric (VA) form factors for the binary semiconductor compounds GaN and InN, with their lattice parameter a (Å)

By injecting the pseudopotential parameters into the EPM code, with values listed in Table (III.1), we determine the energy band gaps, illustrated in Table (III.2). These results exhibit a good agreement with experimental data as reported in references [40,41].

III.2.2. Energy band gap

The variation of direct energy band gap $E_{\Gamma}^{\Gamma}(eV)$ and indirect energy band gap $E_{\Gamma}^{X}(eV)$, $E_{\Gamma}^{L}(eV)$

$\boldsymbol{E\Gamma_{\Gamma}(eV)}$ have been calculated For the different x components of $\mathbf{In_xGa_{1-x}N}$ alloy , ranging from x=0 to x= 1, our results are presented in the Table. (III-2).

Component	$\boldsymbol{E_{\Gamma}^{\Gamma}}$**(eV)**	$\boldsymbol{E_{\Gamma}^{X}}$**(eV)**	$\boldsymbol{E_{\Gamma}^{L}}$**(eV)**
GaN	3.31[a)] 3.3 [b)]	4.58[a)] 4.57[b)]	6 .05[a)] 6 .04[b)]
InN	1.94606 [a)] 1.90 [c)]	2.51754 [a)] 2.8 [c)]	5.82467 [a)] 5.12 [c)]
$In_{0.6}Ga_{0.6}N$	2.30422	3.15139	5.68274

Table III-2: Comparison of the calculated and experimentally measured energy band gaps in the binary semiconductor compounds GaN and InN.

Where:

a) Calculated value, b) Experimental value shown in Ref [40], c) Experimental value given in Ref [41].

We note that our gap results are in better agreement with the experiment.

The variation of the gap $E_{\Gamma}^{\Gamma}(eV)$ of the $\mathbf{In_xGa_{1-x}N}$ alloy as a function of the x composition is shown in Figure (III-1).

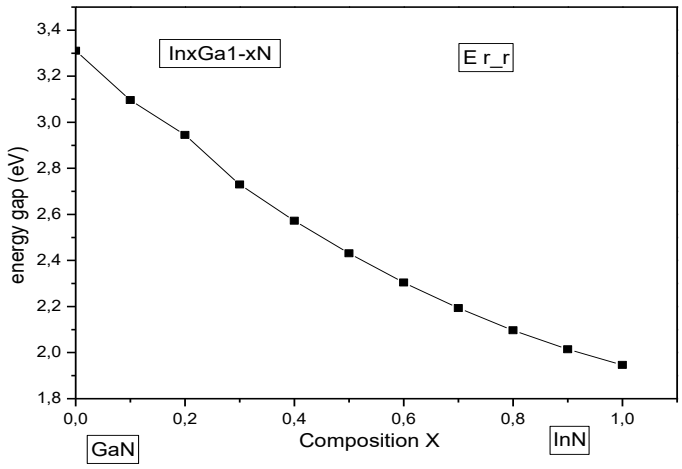

FigureIII-1: The variation of the direct gap $(\boldsymbol{E_I^{\Gamma}})$ of the $\mathbf{In_xGa_{1-x}N}$ Alloy as a function of the composition x

The quadratic interpolation using the least squares method on the curve gives us the following analytic expression:

$$E_{\Gamma}^{\Gamma} = 0.78475x^2 - 2.15173x + 3.31368 \quad (VCA) \tag{III-5}$$

We can see from the curve that the variation is monotonic and decreasing (with the proportion of the indium in the alloy) from 3.31368 eV for the Binary compound GaN to 1.94529 eV for the Binary compound InN. We noted that this characteristic is common in ternary semiconductors such as $\mathbf{In_xGa_{1-x}N}$.

where adjusting the composition allows for precise control of the energy band gap, making it highly advantageous for optoelectronic devices such as LEDs, laser diodes, and solar cells, where specific band gaps are needed for different wavelengths of light.

The variation of the gap $E_X^r\ (eV)$ of the $In_xGa_{1-x}N$ alloy as a function of the x composition is shown in Figure (III2).

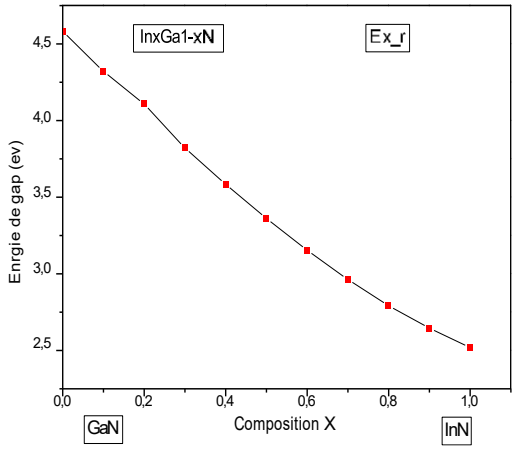

FigureIII-2: The variation of the direct gap $E_X^{\Gamma}(eV)$ alloy as a function of the composition x.

The quadratic interpolation using the least squares method on the curve gives us the following analytic expression:

$$E\Gamma = 0.75254x2 - 2.85353x + 4.60245 \quad \text{(VCA)} \qquad \text{(III-6)}$$

We can see from the curve that the variation is monotonic and decreasing (with the proportion of the indium in the alloy) from 4.60245 eV for the Binary compound GaN to 2.512305 eV for the Binary compound InN.

This energy gap flexibility makes $\mathbf{In_xGa_{1-x}N}$ alloys widely used in optoelectronics, especially in applications such as multicolor LEDs, laser diodes, and solar cells. Their tunable band gap—achieved by adjusting the x composition of the indium in the alloy makes them highly adaptable for devices that demand precise wavelength control.

The variation of the gap $E_X^{\Gamma}(eV)$of the $\mathbf{In_xGa_{1-x}N}$ alloy as a function of the x composition is shown in Figure (III-3).

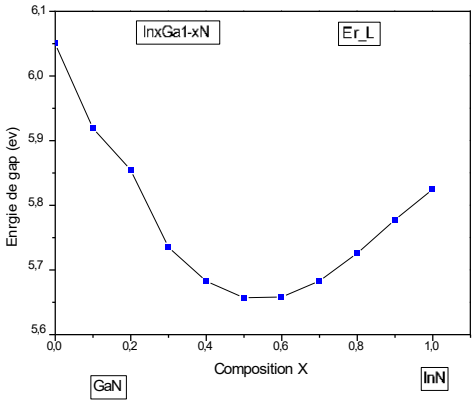

Figure III -3: The variation of the indirect gap (E_L^{Γ}) of the $In_xGa_{1-x}N$ Alloy as a function of the composition x

The quadratic interpolation using the least squares method on the curve gives us the following analytic expression:

$E_L^{\Gamma} = 1.11635x^2 - 1.3175\ x + 6.04673$ (VCA) (III-7)

We can see from the curve that the band gap energy initially decreases as the proportion x of the indium in the alloy ,it increases from x=0 to about x=0.604,It reaches a minimum around x= 0.6, then increases again toward the Binary compound InN .This a nonlinear behavior, is due to the band structure bowing or the interaction effects between InN and GaN states.

The variations in direct band gap E_{Γ}^{Γ}**(eV)** and both indirect band gaps E_X^{Γ} **(eV)** and $E_L^{\Gamma}(eV)$ as a function of composition x without the disorder effect in the ternary alloy $In_XGa_{1-X}N$ **Alloy** are illustrated in Figure (III-4).

.

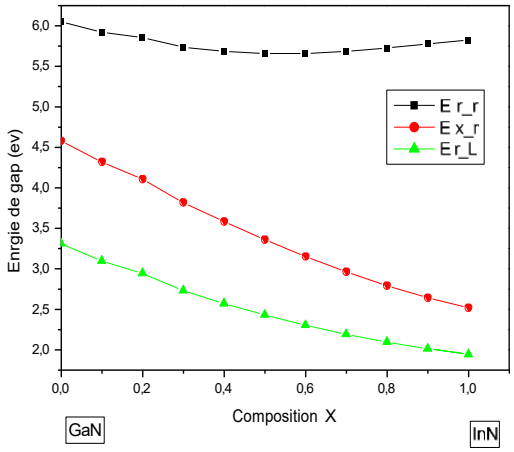

Figure III-4: Variation in direct gap (E_{Γ}^{Γ}) and indirect gaps ((E_{Γ}^{X}), (E_{Γ}^{L})) of the $\mathbf{In_xGa_{1-x}N}$ alloy as a function of composition x.

The graph shows that, when evolving from the binary compound GaN to InN, both the direct band gap energy $E_{\Gamma}^{\Gamma}(x)$ and the indirect band gap energy $E_{x}^{\Gamma}(x)$ exhibit the same behavior as a function of the composition x. All energy transitions decrease with increasing the proportion x of the indium in the alloy, however, the indirect band gap energy $E_{L}^{\Gamma}(x)$shows a mild curvature and remains the highest across all compositions, The latter does not vary linearly with composition x, as it exhibits a pronounced non-linearity due to atomic interactions and strain effects within the material.

This characteristic is essential in optoelectronics, particularly for LEDs, lasers, and solar cells, as it influences light emission properties and device efficiency. Researchers use bowing parameters to optimize performance and tailor materials to different wavelengths

According to our study, we can conclude that the band gaps in the $_{-x}$**N alloy** remains direct for compositions x ranging between $0 \leq x < 1$.

III.2.3. The Energy band gap according to Vegard's law

Vegard's law is an empirical rule stating that the property value of an alloy can be determined from linear interpolation of the property values of the elements. constituting it or in the case of higher alloys, the constituent Compounds [25].

Vegard's law assumes that both components A and B in their pure form have the same crystal structure. Here, a $A_xB_{(1-x)}$ is the Energy band gap of the alloy, Eg A and Eg B are the Energy band gaps of the pure components, and x is the mole fraction of B in the alloy. The law is written in the following form for our alloy:

$$(\mathbf{In_xGa_{1-x}N}) = Egx\mathbf{In} + (1-x) \quad \text{(III-8)}$$

$$Eg\mathbf{In_xGa_{1-x}N} = x.\mathbf{1.9} + (1-x).\mathbf{3.3} \quad \text{(III-9)}$$

As the Energy band gap of the binary alloy follows Vegard's law [10], the values are shown in

Table III- 3

Components	**X**	**Eg(A^0)**
GaN	0	3.3
$In_xGa_{1-x}N$	0.1	3.16
	0.2	3.02
	0.3	2.88
	0.4	2.74
	0.5	2.6
	0.6	2.46
	0.7	2.32
	0.8	2.18
	0.9	2.04
InN	1	1.9

Table III.3: Energy band gap of the semiconductor alloy **$In_xGa_{1-x}N$**

As shown in Curve III- the Energy band gap decreases linearly and monotonically with increasing composition x of the indium.

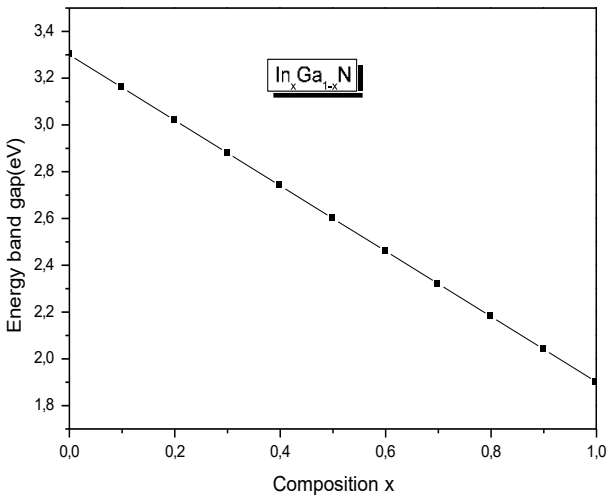

Figure III-5: Variations of the Energy band gap a as a function of the proportion x of Indium according to Vegard's law.

III.2.4. Lattice parameter

The ability to produce ternary, quaternary, or quasi-binary alloys opens up the possibility of producing materials whose band gap width, and therefore optical properties, vary over a very wide range of wavelengths.

The lattice parameter is also a function of the composition, offering greater flexibility in the choice of a particular semiconductor material for a given application depending on the field of use. The choice of the alloy's lattice parameter depends on the composition x, of course, and always remains within the range of the values of the parameters of the parent compounds.

Vegard's law is written in the following form for our alloy as:

$$a\mathbf{In_xGa_{1-x}N} = ax\mathbf{In} + (1-x) \quad \text{(III-10)}$$

$$a\mathbf{In_xGa_{1-x}N} = x.\mathbf{4.98} + (1-x).\mathbf{4.5} \quad \text{(III-11)}$$

As the lattice constant of the binary alloy follows Vegard's law [10], the values are shown in Table III-3:

Components	X	a(A^0)
GaN	0	4.5
$In_XGa_{1-X}N$	0.1	4.548
	0.2	4.596
	0.3	4.644
	0.4	4,692
	0.5	4,74
	0.6	4,788
	0.7	4,836
	0.8	4,884
	0.9	4,932
InN	1	4,98

Table III.4: Lattice parameters of the semiconductor alloy **$In_XGa_{1-X}N$**

As shown in Curve III-5, the lattice parameter a (Å) increases linearly and monotonically with increasing composition x."

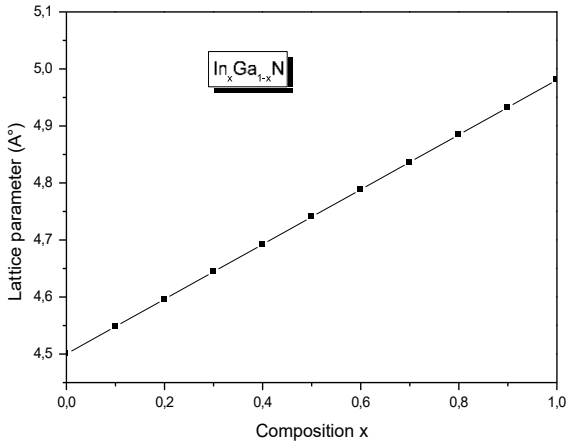

Figure III-6: Variations of the lattice parameter a as a function of the proportion x of Indium according to Vegard's law.

III.2.5. Wavelength

The $In_XGa_{1-X}N$ alloy is a ternary semiconductor composed of indium nitride (InN) and gallium nitride (GaN). Its bandgap varies depending on the indium fraction (x), making it particularly useful for optoelectronic applications.

As shown in Curve III-6 , the variation of the energy band gap energy *E* as a function of wavelength λ for the $In_XGa_{1-X}N$ alloy. Band gap variation ranges from 1.9 eV (InN) to 3.3 eV *(GaN)* where *E* decreases progressively as λ increases. It's clear the ability to adjust the band gap by modulating the indium content, thus facilitating the extension of the material's optical response across the ultraviolet–near-infrared spectrum.

This property makes $In_XGa_{1-X}N$ a highly attractive candidate for a variety of optoelectronic devices operating across a wide spectral domain

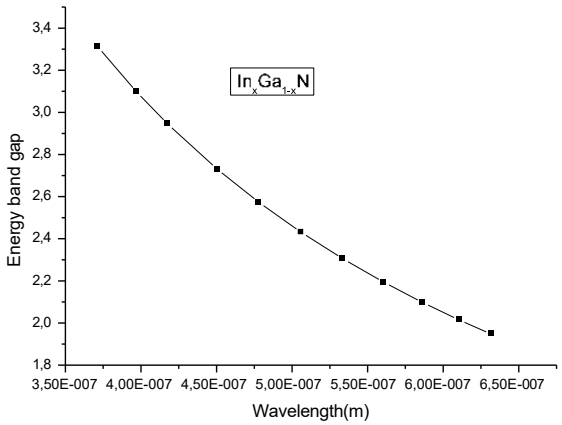

Figure III-7: Variations of the Energy band gap a as a function of the proportion wavelength of Indium according to Vegard's law.

III.2.6 Electronic band structure:

The electronic band structure of the $In_XGa_{1-X}N$ alloy is calculated at points of high symmetry in the Brillouin zone, using VCA without taking into account the effect of compositional disorder.

In order to interpret Figures (III-8, III-9, III- 10), which illustrate the band structures

of binary compound respectively, we note that the zero-energy reference is the valence band maximum.

Figure (III-6) shows that the valence band maximum is at the Γ point and that the conduction band minimum is also at the Γ point, hence the binary compound GaN is a direct bandgap semiconductor. The difference between minimum and maximum is 3.318597 eV, and this coincides with the value reported in reference[28].

On the other hand, Figure (III-7) shows that the valence band maximum is at the Γ point and that the conduction band minimum is also at the Γ point, hence the binary compound InN is a direct bandgap semiconductor. The difference between minimum and maximum is 2.04907 eV, and this coincides with the value reported in reference [28].

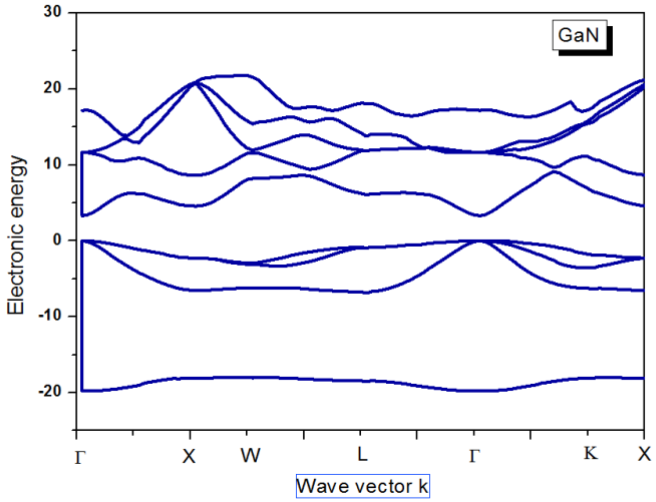

Figure III-8: Electronic band structure of the binary compound GaN

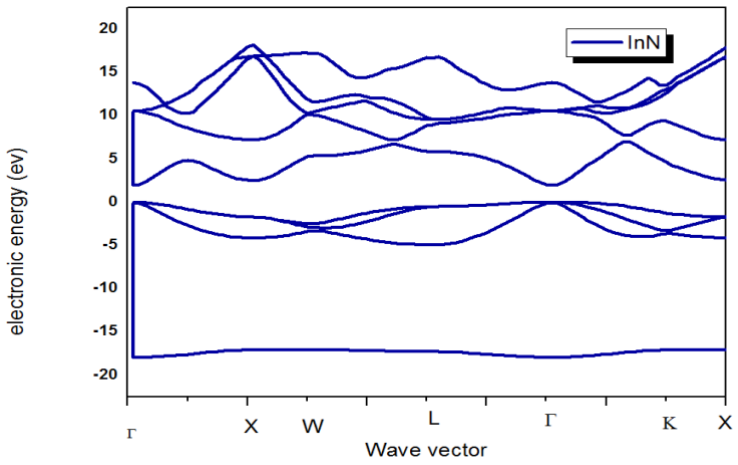

Figure III-9: Electronic band structure of the binary compound InN.

The energy band structure of the ternary $In_{0.6}Ga_{0.4}N$ alloy is shown in figure (III-8) 2.30837 eV from the valence band maximum.

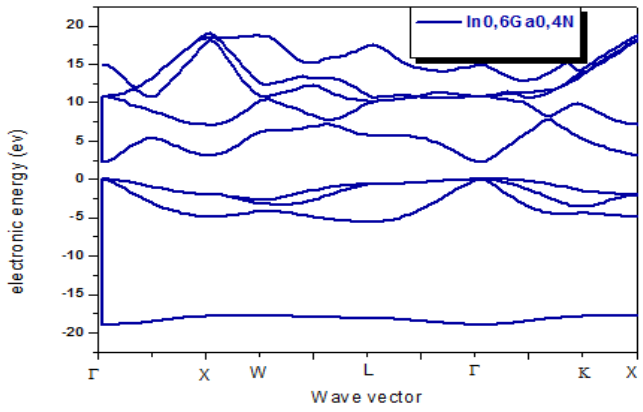

Figure III-10: Electronic band structure of the ternary alloy $In_{0.6}Ga_{0.4}N$

III.3 Study of optical properties:

III.3.1. Refractive index:

The refractive index (n) of semiconductors is a very important physical parameter linked to microscopic atomic interactions, and is often related to gap energy.
Several approaches have been developed to correlate the gap energy of semiconductors with their refractive index.

The correlation between n and Eg has important repercussions on the band structure of semiconductors, and it would be useful to find an acceptable value of n for any material from this relationship.

Estimating this parameter is important for optical waveguides in optoelectronic structures such as heterojunction laser diodes, optical amplifiers and optical Fibers.

There are several models for calculating this parameter, Moss was the first to find a relationship between the refractive index n and the energy gap E_g based on the atomic model, his formula is given as follows

1.Ravindra and Srivastava model

$$n^4 \mathrm{Eg} = k \qquad \text{(III-12)}$$

Where the constant k=108eV is established by Ravindra and Srivastava [29].

2.Gupta and Ravindra model

The linear form of Gupta and Ravindra [30]

$$n = \alpha + \beta E g \qquad \text{(III-13)}$$

Where α =4.084 and β= -0.62 eV^{-1}

3.Hervé and vandamme model

The empirical relationship of Hervé and Vandamme given by [31]:

$$n = \sqrt{1 + \left(\frac{A}{E_g + B}\right)^2} \qquad \text{(III-14)}$$

With A=13.6 eV et B=3.4 eV

4.Reddy Anjaneyulu's model

Reddyat Anjaneyulu's relationship [32]

$Ege^n = 36.3$ (III-15)

5.Ravindra model

Ravindra's linear form [33].

$n = \alpha + \beta Eg$ (III-16)

6.Reddy et Ahammed model [24]

$n^4(E_g - 0.365) = 1.54$

Using these six models, we have calculated the refractive index of $\mathbf{In_xGa_{1-x}N}$ semiconductor alloys from the values of their energy gaps.

Our refractive index calculation results for each model are shown in Table (III-4).

	Composition x	$n_{1(Model1)}$	$n_{2(Model2)}$	$n_{3(Model3)}$	$n_{4(Model4)}$	$n_{5(Model5)}$	$n_{6(Model6)}$	N_{exp}
GaN	0	2.39	2.0318	2.26	2.4031	1.3465	0.8503	2.3[a)]
	0.1	2.4301	2.1641	2.32	2.4697	1.528	0.8665	
	0.2	2.4609	2.2583	2.3653	2.52	1.657	0.879	
	0.3	2.5079	2.3913	2.4335	2.5957	1.8394	0.8983	
	0.4	2.5455	2.4892	2.4871	2.6553	1.9736	0.9139	
	0.5	2.5818	2.5771	2.5379	2.7119	2.0941	0.9292	
	0.6	2.6165	2.6553	2.5854	2.7653	2.2014	0.944	
	0.7	2.649	2.7243	2.6292	2.8147	2.2959	0.958	
	0.8	2.6791	2.7842	2.668	2.8598	2.3781	0.9711	
	0.9	2.706	2.8353	2.7037	2.8999	2.4481	0.983	
InN	1	2.7293	2.8684	2.7334	2.9342	2.5058	0.9934	2.9[a)]

Table III.5: Refractive index (n) of GaN, $\mathbf{In_xGa_{1-}}$ and InN semiconductors using different models.

Where:

a) Theoretical value indicated in Ref [M. Levinshtein, S. Rumyantsev, M. Shur Eds.), Handbook Series on Semiconductor Parameters, vol. 2, World Scientific, Singapore, (1999).]

To make a comparison, we have also presented the theoretical value cited in reference (a), It follows from these comparisons that, the best agreement between our results and the theoretical value according to the following relationship:

$\Delta n = \frac{n_{exp} - n_{calc}}{n_{exp}}$ as shown in Table III-5.

	Δn_1	Δn_2	Δn_3	Δn_4	Δn_5	Δn_6
GaN (X=0)	0.03913	0.116608	0.0173913	0.044826	0.4145652	0.6303043
InN (X=1)	0.058862	0.01089655	0.05744827	0.011793	0.1359310	0.657448275

Table III-6: comparison of calculated values and experimental data

The best agreement between our results and the theoretical value of compound **GaN** is given by the relations of the models of both **Ravindra and Srivastava** and **Reddy and Anjaneyulu**.

But it must be said that the model that gives the closest value to the theoretical value is the **Reddy and Anjaneyulu** model.

The best agreement between our results and the theoretical value of compound **InN** is given by the relations of the model of **Reddy and Anjaneyulu**.

Then we can conclude that the **Reddy and Anjaneyulu** is the most appropriate model for our ternary alloy $\mathbf{In_XGa_{1-x}}$.

Figure (III-9) shows the variation in the refractive index of $\mathbf{In_XGa_{1-X}N}$ as a function of indium composition x for the six models

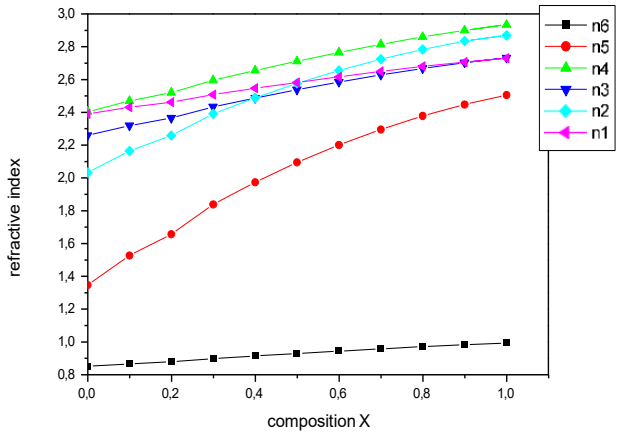

Figure III-11: Variation in the refractive index of $\mathbf{In_XGa_{1-x}N}$ as a function of indium composition x for the six models.

We observe that all models show the same behavior, with the refractive index increasing with increasing indium x composition. The increase in refractive index is directly linked to the value of the gap as a function of composition x. It increases as the gap decreases.

III.4 Study of dielectric properties

III.4.1 High-frequency dielectric constant

Knowing (n) allows us to calculate the high-frequency dielectric constant ε∞ which is considered a crucial parameter in the design of optical devices. For this purpose, the high-frequency dielectric constant ε∞ will be calculated from the following expression: $\varepsilon\infty = n^2$ III.

After opting for the Reddy and Anjaneyulu model for the calculation of the refractive index (n), the values of the high-frequency dielectric constant ε∞for GaN and InN are 5.77 and 8.61, respectively.

Compared with the experimental values of 5.75 for (GaN) and7.1 for (InN) cited in Ref. [a], our results seem to be consistent with those of Ref. [a].

Due to the limited available data on the high-frequency dielectric constant ε_∞ for $\mathbf{In_XGa_{1-X}N}$ in the literature, our result will serve as a reference for future investigations. The variation of the high-frequency dielectric constant ε_∞ as a function of the indium concentration of the ternary alloys $\mathbf{In_XGa_{1-X}N}$ is plotted in Figure III-12. It should be noted that with increasing indium Concentration, ε_∞ increases monotonically, the behavior of ε_∞ is same to that of x and also similar to that of n.The variation of ε_∞ as a function of x indicates that as soon as one proceeds from GaN (x = 0) to InN (x = 1), the ternary alloy of interest (0 <x <1) progressively becomes a good electrical insulator .

.

	$\varepsilon_{\infty} = n^2$	ε_∞ exp
GaN (x=0)	5.77	**5.75** a)
$In_{0.5}Ga_{0.5}N$ (x=0.5)	7.35	
InN (x=1)	8.61	7.1 a)

Table III-7: comparison of calculated values and experimental data.

The graph shows the dependence of the high-frequency dielectric constant on the composition parameter x. It is observed that the high-frequency dielectric constant increases progressively with the increase in composition. Starting from approximately $\varepsilon\infty = 5.77$ at x=0 (GaN), the high-frequency dielectric constant index rises progressively and reaches about $\varepsilon\infty = 8.61$ at x= 1 (InN).

This monotonic and nearly linear trend indicates that the optical density of the alloy becomes higher as the proportion of one of its components increases. Such behavior is typical in semiconductor

or optical materials, where altering the chemical composition allows for the tuning of optical properties like light absorption, reflectivity, and transmission.

This relationship is crucial for designing materials with specific optical characteristics, especially in applications like photodetectors, solar cells, LEDs, and waveguides.

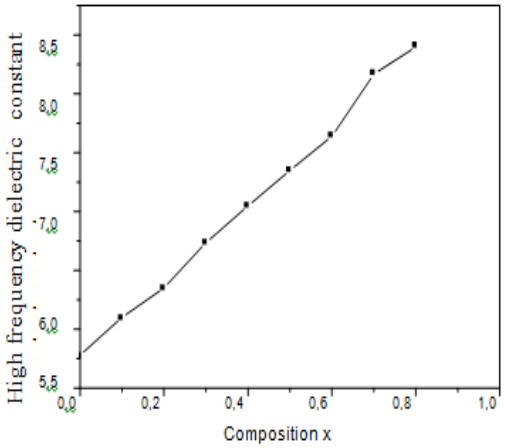

Figure III-12: The variation of the high frequency dielectric constant of the alloy $\mathbf{In_xGa_{1-x}N}$

III.5 CONCLUSION

In this chapter we have investigated the electronic, optical and dielectric properties, such as energy gap, refractive index and high-frequency dielectric constants, of the ternary semiconductor alloyInxGa1- xN. To this end, we used the empirical pseudopotential method coupled to the virtual crystal approximation. All properties were examined as a function of indium composition x.

In the two binary compounds GaN, InN. $\mathbf{In_xGa_{1-x}N}$ alloy is direct-gap for all indium concentrations.

The refractive index was calculated according to six existing models, varying monotonically and linearly with indium composition x. This behavior is similar for the variation of high-frequency dielectric constants as a function of indium composition x.

General conclusion

General conclusion

In this work, we set out to understand the structural, electronic, optical and dielectric properties of ternary $In_xGa_{1-x}N$ semiconductor alloys. All these properties have been examined as a function of indium x composition. Calculations are mainly performed using the EPM empirical pseudopotential method, coupled with the VCA virtual crystal approximation.

Our results show that for $In_xGa_{1-x}N$, with lattice parameters ranging from 4.5 Å (GaN) to 4.98 Å(InN).

A direct gap ($\boldsymbol{E_\Gamma^\Gamma}$) and with a considerable deviation from the gaps ($\boldsymbol{E_X^\Gamma}$),($\boldsymbol{E_L^\Gamma}$) and that no gap transition is noticed. Its value varies from 3.31eV to 1.94606 eV whenever x varies from 0 to 1. The direct gap decreases with increasing composition x, this variation is monotonic and linear. And the decrease in indirect gaps ($\boldsymbol{E_X^\Gamma}$), ($\boldsymbol{E_L^\Gamma}$)with increase in composition x this variation is also monotonic and linear.

The refractive index was calculated according to six empirical models. The variation of refractive index as a function of composition x for the ternary semiconductor alloy InxGa1-xN shows an increase in refractive index with increasing indium composition x for all models used. With InN and GaN compounds, the best agreement between our results and the theoretical value is that given by the Ravindra and Srivastava model and Reddy Anjaneyulu's model gives the value that is closest to the theoretical value

The high-frequency dielectric constant ε_∞ is calculated for the best model, their behavior as a function of indium composition x is the same, monotonic and linear.

Controlling these parameters by varying the x composition of the ternary InxGa1-xN alloy is of paramount importance for the design of new optoelectronic devices.

Bibliographical references

[1] Boubtana Khayra, et Fedjer Rachida, “Mémoire de Master Etude des propriétés structurale et électronique d‟un matériau semi-conducteur III-V(AlGaN)” Université – Tissemsilt, (2015).

[2] Kara Mohemed Wahiba, “Thèse de doctorat Etude Les structures de bandes électroniques et les propriétés relatives aux semiconducteurs quasi binaires (GaP)1-x(ZnSe)x” Université Mohemed Khider – Biskra, (2011). **[3]** Abderrachid Bechir, “Thèse de Doctorat D‟état Effets du désordre et du substrat sur la Structure électronique” Université Mentouri – Constantine, (2006).

[4] F. Mezrag, Thèse de doctorat, Univ Mohamed Khider Biskra (2012)

[5] Kara Mohamed Wahiba, "Doctoral Thesis: Study of Electronic Band Structures and Properties Related to Quasi-binary Semiconductors $(GaP)_{1-x}(ZnSe)_x$", Mohamed Khider University – Biskra, (2011).

[6] Julien Sellés, "Optical Spectroscopy of GaN/AlN Nanostructures in Planar Microcavities and Microdisks. Physics [physics]", University of Montpellier, (2015). In French.

[7] BERBER Mohamed, "Doctoral Thesis: Study of Laser Nanostructures Based on GaNSb/AlGaInNSb Antimonide Nitrides", Djilali Liabes University – Sidi Bel Abbes, (2014).

[8] Mme Laiadi Widad, "Doctoral Thesis: Numerical Simulation of the Effect of the $Al_xGa_{1-x}As$ Window Layer on the Resistance to Space Irradiations of a Gallium Arsenide (GaAs) Solar Cell", Mohamed Khider University – Biskra, (2014).

[9] Nasouri Mesbah, "Master's Thesis: Simulation Study of AlGaN/GaN Structures for HEMTs", Saad Dahleb University – Blida, (2011).

[10] Mr Nassim Touka, "Doctoral Thesis: Dispersion of Semiconductor Nanocrystals in Wide Band Gap Matrices: Study of Optical Properties", Mentouri University – Constantine, (2010).

[11] Boubtana Khayra and Fedjer Rachida, "Master's Thesis: Study of Structural and Electronic Properties of a III-V Semiconductor Material (AlGaN)", University of Tissemsilt, (2015).

[12] F. Languy, *Ph.D. Thesis*, University Faculties of Notre-Dame de la Paix, Faculty of Sciences of Namur, 2007.

[13] V.L. Solozhenho, in: J.H. Edgar (Ed.), Properties of Group III Nitrides, Electronics

Materials Information Service (EMIS) Data Reviews Series, Institution of Electrical Engineers, London, 1994.

[14] A. Trampert, O. Brandt, K.H. Ploog, in: J.I. Pankove, T.D. Moustakas (Eds.), Crystal Structure of Group III Nitrides Semiconductors and Semimetals, Vol. 50, Academic Press, San Diego, 1998.

[15] WorldLingo, "Indium Gallium Nitride", [Online]. Available.

[16] *Handbook of Nitride Semiconductors and Devices*, Vol. 1, 2008.

[17] Fella Benmakhlouf, "Doctoral Thesis: Theoretical Investigation of Electronic and Structural Properties of II-VI Semiconductor Alloys under Normal and High Pressure", Mentouri University – Constantine, (2006).

[18] Abderrachid Bechir, "State Doctorate Thesis: Effects of Disorder and Substrate on Electronic Structure", Mentouri University – Constantine, (2006).

[19] H. Hamzaoui, *Sol. Energy Mater. Sol Cells*, vol. 87, pp. 595–603, 2005.

[20] O. Ambacher, *J. Phys. D: Appl. Phys.*, vol. 31, pp. 2653–2710, 1998.

[21] M. Mostfaoui, *Magister Thesis*, University of Sidi Bel Abbes, 2010.

[22] Th. Gessmann, Y-L. E. L., E.L. Waldron, J. W. Graff, E. F. Schubert, and J.K. Sheu, *Journal of Electronic Materials*, vol. 31, no. 5, 2002.

[23] A. Martí, C. Tablero, E. Antolí, A. Luque, R. P. Campion, S. V. Novikov, C.T. Foxon, *Sol. Ener. Mater. Sol. Cell*, vol. 93, pp. 641–644, 2009.

[24] Handbook of Nitride Semiconductors and Devices, Vol. 1, 2008.

[25] G. F. Brown, J. W. Ager, W. Walukiewicz, J. Wu, *Sol. Ener. Mater. Sol. Cell*, vol. 94, pp. 478–483, 2010.

[26] W. J. Aziz, K. Ibrahim, *J. Nan Electronics and Materials*, vol. 3, pp. 43–52, 2010.

[27] Md. Tanvir Hassan, Ashraful G. Bhuiyan, Akio Yamamoto, *Solid-State Electronics*, vol. 52, pp. 134–139, 2008.

[28] Bechiri, Abderrachid, *Effects of Disorder and Substrate on the Electronic Structure*.

[29] Bahi, Wafa, *Binary Semiconductors Used in Optoelectronic Components*.

[30] John H. Davies, The physics of low-dimensional Semiconductors, Cambridge University Press, (1998**)**

[31] Schrödinger, E. (1926). *Quantisierung als Eigenwertproblem* (First and Second Papers). **Annalen der Physik**, *79*, 361–376; 489–527.)

[32] M. Born, R. Oppenheimer, Ann. Physik., 84, 457, (1927).

[33] J. Chelikowsky and M. L Cohen Phys. Rev B14, 552 (1976).

[34] P. Y. Yu and M. Cardona, Fundamentals of semiconductors: physics and materials properties, springer-Verlag, Berlin Heidelbeg New-York (2001).

[35] C. Herring, Phys. Rev. 57, 1169 (1940).

[36] D. Brust, J. C. Phillips and F.Bassani, Phys. Rev. Lett. 9, 94 (1962).

[37] I. V. Abarenkov and V. Heine, Phil. Mag. 13, 529 (1965).

[38] H. Hellmann, W. Kassatotschkin, Acta Physicochim. U.R.S.S. 5, 23 (1936).

[39] J. C. Phillips and L. Kleinman, Phys. Rev. 116, 287 (1959).

[40] J. C. Phillips. Phys. Rev. 112, 685 (1958); F. Bassani and V. Celli, J. Phys. Chem. Solid 20, 64 (1961); M. L. Cohen and V. Heine, Phys. Rev. 122, 1821 (1961); B. I. Austin, V. Heine and L. I. Shen, Phys. Rev. 127, 276 (1962).

[41] M. L. Cohen and V. Heine, Solid State Physics 24, Eds, H. Enrenreich, F. Seitz and D. Turnbull , Academic press, New-York (1970).

[42] M. L. Cohen and T. Bergestresser Phys. Rev. 141, 789 (1966); Références bibliographique M. L. Cohen and T. Bergestresser Phys. Rev. 164, 1069 (1976).

[43] J. R. Chelikowsky and M. L. Cohen, Phys. Rev. Lett. 32, 674 (1974); W. A. Harrisson, Phys. Rev. B14, 702 (1976).

Résumé :

Le but de ce travail est d'étudier les propriétés électroniques, optiques et diélectriques et la masse effective de l'alliage ternaire semi-conducteur $In_xGa_{1-x}N$ dans la structure zinc blende Ces alliages ont un intérêt important pour la conception des dispositifs optoélectroniques. Les calculs sont principalement basés sur l'approche du pseudo-potentiel empirique combinée avec l'approximation du cristal virtuel VCA.

Nos résultats ont montré qu'en faisant varier la concentration de l'indium, l'alliage $In_xGa_{1-x}N$ présente un gap direct pour l' intervalle $(0 \leq x \leq 1)$ .Ce travail pourrait nous fournir des diverses possibilités pour l'obtention des indices de réfraction et des constantes diélectriques en faisant varier le compositions x.

Nos résultats sont en bon accord avec d'autres résultats expérimentaux et théoriques.

Mots clés : Les semi-conducteurs III-V. l'alliage $In_xGa_{1-x}N$.l'approximation du cristal virtuel VCA, pseudo-potentiel empirique EPM.

Abstract

The aim of this work is to study the electronic, optical and dielectric properties and the effective mass of the ternary semiconductor alloy $In_xGa_{1-x}Sb$ in the zinc blende structure. These alloys have an important interest for the design of optoelectronic devices. The calculations are mainly based on the empirical pseudo-potential approach combined with the VCA virtual crystal approximation.

Our results have shown that by varying the concentration of indium, the $In_xGa_{1-x}N$ alloy presents a direct gap for the interval $(0 \leq x \leq 1)$. This work could provide us with various possibilities for obtaining refractive indices and dielectric constants by varying the composition x.

Our results are in good agreement with other experimental and theoretical results.

Keywords :

semiconductors III-V. the alloy $In_xGa_{1-x}N$. The virtual crystal approximation VCA, empirical pseudo- potential EPM.

الملخص:

الهدف من هذا العمل هو دراســة الخواص إلكترونية والضــوئية والعازلة والكتلة الفعالة لســبائك أشــباه الموصــلات الثالثي InxGa1-xN في هيكل مزيج الزنك، وهذه الســبائك لها أهمية كبيرة في تصــميم الأجهزة الالكترونية الضــوئية. تعتمد الحسابات بشكل أساسي على نهج إمكانات الزائفة التجريبية جنبا إلى جنب مع التقريب البلوري االافتراضي .VCA أظهرت نتائجنا أنه من خلال تغيير تركيز الند يوم، تقدم ســبيكة InxGa1-xN فجوة مباشــرة للمجال 0(≥ x يمكن أن يوفر لنا هذا العمل إمكانيات مختلفة للحصول على مؤشرات االإنكسار وثوابت العزل الكهربائي عن طريق تغيير تكوين x